

AI for Calcium Scoring

Sanne G.M. van Velzen^{1,2}, Nils Hampe^{1,2}, Bob D. de Vos^{1,2}, and Ivana Išgum^{1,2,3}

¹Department of Biomedical Engineering and Physics, Amsterdam University Medical Centers - location AMC, University of Amsterdam, the Netherlands

² Amsterdam Cardiovascular Sciences, Amsterdam University Medical Centers, the Netherlands

³Department of Radiology and Nuclear Medicine, Amsterdam University Medical Centers - location AMC, University of Amsterdam, the Netherlands

Abstract. Calcium scoring, a process in which arterial calcifications are detected and quantified in CT, is valuable in estimating the risk of cardiovascular disease events. Especially when used to quantify the extent of calcification in the coronary arteries, it is a strong and independent predictor of coronary heart disease events. Advances in artificial intelligence (AI)-based image analysis have produced a multitude of automatic calcium scoring methods. While most early methods closely follow standard calcium scoring accepted in clinic, recent approaches extend this procedure to enable faster or more reproducible calcium scoring. This chapter provides an introduction to AI for calcium scoring, and an overview of the developed methods and their applications. We conclude with a discussion on AI methods in calcium scoring and propose potential directions for future research.

Keywords: Calcium score, CT, machine learning, deep learning, artificial intelligence

1 Introduction

Cardiovascular disease (CVD) accounts for approximately one-third of all global deaths [1]. With obesity being a global health concern, worldwide rates of diabetes mellitus on the rise, and an increasing number of smokers in developing countries, the need for early detection of CVD risk is increasingly apparent.

Calcium scoring, a process in which arterial calcifications are detected and quantified in CT, has been shown to be valuable in prediction of cardiovascular events [2]. For instance, calcifications in the aortic arch and carotid arteries have been associated with an elevated risk of stroke [3,4]. The amount of coronary artery calcification (CAC) is a strong and independent predictor of coronary heart disease (CHD) events[5,6] and therefore, calcium scoring is most often applied to the coronary arteries.

Calcium scoring is standardly performed in CT scans without contrast enhancement, where lesions are defined as a high density area of ≥ 130 Hounsfield

Units (HU) in an artery[7]. Calcifications are standardly quantified into Agatston, volume and mass scores [8]. The volume score represents the volume of calcified lesions and it only takes the voxel size into account, while the calcium mass considers both the volume and the density of the lesions. Both scores are used for quantification of calcifications in any artery, while the Agatston score is applied to the coronary arteries only. The Agatston score is a slice based quantification method that combines the area of a lesion with an ordinal weight term based on the maximum density of the lesion in each slice ($< 200\text{HU}$: 1; $< 300\text{HU}$: 2; $< 400\text{HU}$: 3; $\geq 400\text{HU}$: 4). The total Agatston score is obtained by summing the 2D lesion scores over all slices. Based on the total Agatston score a patient can be assigned to a risk category that directly relates to a 10 year risk of CVD events [7,9]. Commonly used risk categories are listed in Table 1.

Table 1. Commonly used risk categories based on Agatston scores determined in the coronary arteries.

Agatston score	Risk
0	very low
1-10	low
11-100	intermediate
100-400	high
>400	very high

1.1 Standard calcium scoring

Routinely, only coronary calcium scoring is performed. In clinic, this is done with commercially available software in a semi-automatic manner. The interactive software projects an overlay showing all the areas above 130 HU onto a CT slice. Subsequently, the areas in the coronary arteries representing CAC are manually identified by the expert with a mouse click. The software then automatically identifies the whole lesion and labels it according to the artery label provided by the expert. This process is repeated for each CAC lesion and each CT slice. Thereafter, the identified lesions are quantified into Agatston score, volume and mass. The scores are calculated per artery and over all arteries.

1.2 AI for calcium scoring

Although manual calcium scoring is not considered a difficult task for experts, it can be tedious and time consuming, especially when large numbers of scans are involved or the image quality is compromised. Therefore, a multitude of artificial intelligence (AI) methods have been developed to automate calcium scoring [10,11].

Due to large variability in the manifestation of calcified plaque and its look-alikes, designing rule-based algorithms for identifying calcified plaque is far from

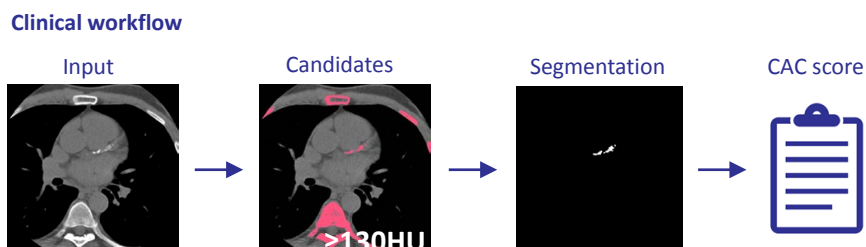


Fig. 1. Clinical workflow for CAC quantification: Lesion candidates are extracted based on their image intensity values and thereafter, the arterial calcifications of interest are identified and quantified.

trivial. Instead, state-of-the-art automatic systems utilize machine learning to learn the intuitive rules experts apply when scoring a scan. Calcium scoring is often posed as a classification problem where the machine learning task is to separate arterial calcifications from their lookalikes. In conventional machine learning, classification is performed based on the information describing the potential calcifications (features) that is relevant for the task at hand. In case of calcium scoring the potential calcifications typically consist of candidate lesions above 130 HU in the scan, that need to be classified into calcifications or other lesions. The features used in automatic calcium scoring typically describe lesion size, shape, texture and location in the scan. For calcium scoring it is feasible to obtain labels for the training data, i.e. for each candidate lesion a label can be obtained that indicates whether the lesion is a true arterial calcification or not. Hence, the training of calcium scoring methods is supervised: the classifier learns to perform the classification based on labeled example data. When training is finished, the free parameters are frozen and the algorithm can be used to classify previously unseen samples.

While extensive research throughout multiple decades has produced a wide spectrum of machine learning algorithms, hardware and algorithm developments over the last years evoked the creation of an entirely new AI category, termed deep learning. The most distinct difference between deep learning and the conventional machine learning algorithms lies in their ability to learn directly from the data, circumventing the need for designing features. This shifts the focus from carefully designing specific features that incorporate expert knowledge about the task at hand to engineering the network architecture and the optimization process. Furthermore, ability of deep learning approaches to learn optimal features simultaneously with the classification can result in substantially improved performance. Like in calcium scoring using conventional machine learning, deep learning calcium scoring methods predominantly utilize supervised approaches.

We discuss machine learning and deep learning methods for calcium scoring that follow standard identification of calcified lesions in clinic in Section 2. Later methods advance coronary calcium scoring to achieve faster and more reproducible measurements. These methods are discussed in Section 3. Finally,

Section 4 provides a discussion on the current state of the art and potential future research directions.

2 Automatic coronary calcium scoring

To date, most automatic coronary calcium scoring methods are closely related to the expert manual calcium scoring procedure using commercial software solutions: Lesion candidates are first extracted based on their image intensity values and thereafter, the calcifications of interest are identified (Fig. 1). Currently, most automatic CAC scoring methods focus on automating the manual lesion identification with a machine learning classifier or deep learning architecture.

In clinical practice, only coronary calcium scoring is routinely performed and it is done in dedicated calcium scoring CT (CSCT) scans. However, other CT protocols that visualize the heart also allow CAC scoring. Because different CT protocols pose different challenges, we describe automatic CAC scoring per target CT protocol.

2.1 Coronary calcium scoring in cardiac CT

For quantification of CAC, a dedicated CSCT is performed without contrast enhancement, with electrocardiography (ECG)-triggering, 120 kVp and 3 mm slice thickness [12]. The dedicated protocol allows for optimal visualization of coronary calcifications and hence, accurate quantification of CAC. Absence of contrast agent in the arteries allows for good visualization of the calcified lesions. Moreover, the slice thickness of 3 mm minimizes image noise and therefore allows discrimination between small calcifications and noise voxels. Furthermore, using ECG, image acquisition is triggered to the end-diastolic phase, when the heart is most stable. Minimizing cardiac motion is particularly important for coronary calcium scoring due to its pronounced effect on visualization of the coronary arteries.

Analogous to clinical calcium scoring, earliest AI methods for coronary calcium scoring were generally focused on application in CSCT scans, in which they computed a total CAC score. The typical automation pipeline of these early methods starts with defining the region of interest (ROI). In the defined ROI, the methods identify true calcified lesions among a set of candidates using a supervised machine learning classifier based on handcrafted features [13,14,15,16,17,18].

Published methods mainly differ in strategies for defining the region of interest (ROI), the choice of machine learning classifier and the type of computed features. A combination of classifiers typically led to the best performance [13,14]. Išgum et al [13] used k-nearest neighbor (kNN) classifiers sequentially, where the result of the first classifier was used as input to the second classifier: In the first stage, obvious positives and obvious negatives were discarded, and, subsequently, a new classifier was trained for the remaining, more difficult candidates [13]. Alternative to such a sequential combination, Kurkure et al. [14] proposed to merge

the output of an ensemble of multiple support vector machine (SVM) classifiers that were trained separately on different independently sampled subsets of the training data. This way a robust method was trained.

Next to the classifier, the computed features played an essential role in the automation pipeline. Features often describe shape, size, appearance and location of calcium lesions [13,14,15,16,17,18]. While shape, size and appearance features are described directly from the lesions using for instance volume, Gaussian filters and intensity value statistics, their spatial location requires contextual information from the scan. For instance, Işgum et al.[13] described the position of lesions with respect to anatomical structures, i.e. the heart and the aorta. Kurkure et al. [14] defined location features relative to a bounding box around the heart. The features were agnostic to the specific machine learning classifier and their descriptive power was crucial for algorithm performance.

Besides location information being important for distinguishing true coronary calcifications among candidates, it is useful for computing per artery scores. Therefore, machine learning methods were proposed that, unlike the aforementioned methods, used location information to infer in which coronary artery a lesion may reside in. Brunner et al.[16] used coordinates with respect to manually placed landmarks as features to assign all voxels in a CSCT scan to classes belonging to one of the three main coronary artery branches (LAD, LCX and RCA) or background with an SVM. By assigning lesion candidates to the predicted coronary artery, artery specific calcium scoring was performed. Other methods utilized an additional set of coronary CT angiography scan (CCTA) scans, in which an intravenously administered contrast agent enables visualization of the arteries [17,18]. The CCTA scans were used to define coronary artery atlases, i.e. probabilistic maps of artery locations in typical heart anatomies. Registration of these atlases to CSCT images allowed for obtaining estimates of the coronary artery location and assigning a lesion to an artery. In addition to enabling the computation of artery specific calcium scores based on the CCTA atlases, Shahzad et al. [17] also exploited artery locations in the form of an additional location feature relative to the arteries. Due to the differences in contrast between CCTA and CSCT, accurate registration is a very challenging task. Therefore, Wolterink et al. [18] proposed to first transfer the CCTA atlases to CSCT atlas scans. The hereby obtained CSCT atlases were subsequently used to estimate artery locations. Moreover, the impact of potential registration errors on classification performance was mitigated by computing location features with respect to all coronary arteries instead of merely the closest one. Furthermore, the authors enabled an additional opportunity for a semi-automatic workflow, in which high uncertainty output of the trained classifier was presented to an expert for potential correction. By referring only lesion candidates with high classifier uncertainty, performance similar to a second observer was achieved, with relatively little manual expert input [18].

Recently, deep learning methods have been proposed for CAC scoring in CSCT. Martin et al. [19] segmented the territories in CSCT that belong to the three main coronary arteries with a segmentation convolutional neural network

(CNN). Subsequently, only candidate lesions in the vicinity of the coronary arteries were classified using a neural network that combines spatial coordinate features with features from the segmentation CNN. Van den Oever et al. [20] proposed an approach that employs a CNN to segment CAC by analyzing image slices in three orthogonal directions and thereafter, combines them to obtain the final segmentation. The evaluation showed that due to the absence of false negative predictions, the method could be used to exclude scans without CAC to relieve the workload of radiologist.

Although direct comparison of attained performances by the presented methods is generally desirable, it is often not possible due to differences in evaluation metrics and used datasets. Therefore, Wolterink et al. [21] organized the orCaScore challenge that provided a set of multi-center and multi-vendor training and test CSCT and CCTA scans and a standardized evaluation of the results. At the workshop that launched the challenge, the performance of five (semi-)automatic calcium scoring methods aimed at CSCT was assessed, including the methods of Shahzad et al. [17] and Wolterink et al. [18]. The authors found that, on a lesion level, some methods can identify CAC in CSCT with a sensitivity and positive predictive value close to that of expert observers. Nevertheless, all evaluated methods made common errors, typically at the coronary ostia, where the exact starting point of the coronary arteries is potentially ambiguous, and in distal segments of the coronary arteries, that are difficult to extract with most coronary artery tracking methods.

2.2 Calcium scoring in non-contrast CT showing the heart

Over 7 million non-contrast chest CT scans are annually acquired for clinical care in the United States alone. This amounts to approximately 10 times more acquired chest CT scans than dedicated CSCT scans [22]. Moreover, if lung cancer screening with chest CT would be considered, potentially another 7 to 10 million low-dose chest CTs per year would be acquired [23]. Furthermore, non-contrast CT scans showing the chest are made for non-diagnostic purposes, e.g. radiotherapy treatment planning CT. All these scans visualize the heart and allow calcium scoring in the coronary arteries and in the aorta (Fig. 2). Given the clinical relevance of CAC scoring, the guidelines of the Society of Cardiovascular Computed Tomography and the Society of Thoracic Radiology [12] recommend to quantify and report CAC on *all* such CT scans.

However, a number of extra challenges arise that are not present in CSCT. Since these scans are made for a wide variety of clinical indications, the field of view is not focused on the heart but contains a larger volume, which necessarily translates to a lower in-plane resolution. Moreover, such CT scans are usually acquired without ECG-triggering, resulting in more pronounced cardiac motion artefacts impacting the appearance of calcifications in the coronary arteries.

Nevertheless, also in these scans calcium scoring has most frequently been applied to the coronary arteries. Because localization of the coronary arteries is not feasible due to lack of contrast enhancement and cardiac motion artefacts, machine learning methods for CAC scoring often simplify the analysis by

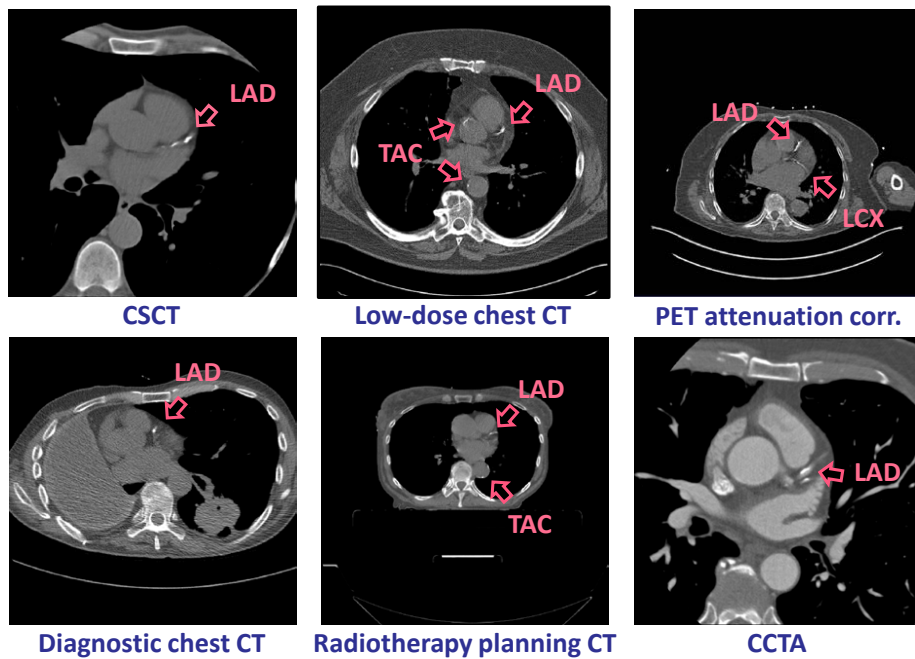


Fig. 2. Examples of different CT scan protocols with pronounced differences in field of view, image resolution, cardiac motion, intravenous contrast and pathology. The arrows indicate calcified lesions in the left anterior descending (LAD) and left circumflex (LCX) artery, and thoracic aorta calcification (TAC).

defining a ROI or incorporate spatial information. For instance, González et al. [24] defined a bounding box around the heart to determine the ROI using machine learning classifiers that classified the presence of the heart per slice in 3 orthogonal directions. Thereafter, a rule based approach was used to classify CAC lesions within the bounding box. Other methods did not specifically restrict the analysis to a certain ROI, but incorporated spatial information in a different manner. Išgum et al. [25] explicitly utilized the property that coronary calcifications appear at typical locations in the coronary artery tree. Through image registration of scans with reference segmentations of CAC, a spatial CAC probability map was created that was used to compute spatial features for candidate calcifications. Like in the methods for CAC detection in CSCT, features describing shape, size, appearance and location of the lesion were computed. These were used to detect CAC lesions with a combination of classifiers. Although the method was developed for low-dose chest CTs, the same method was also applied to attenuation correction CT scans for cardiac perfusion PET scans

[26] and radiotherapy planning CT scans of breast cancer patients [27], both with good agreement with reference scores [28].

Owing to the typically large field of view, these scans also allow quantification of extracardiac arterial calcification in for instance the thoracic aorta, innominate artery or carotid arteries. Accordingly, several automatic methods for extracardiac calcium scoring have been developed. For instance, Išgum et al. [29] proposed to quantify calcifications in the thoracic aorta by delineating the aorta using a multi-atlas segmentation approach and classifying candidate lesions within this volume with two sequential kNN classifiers. Similarly, Chellamuthu et al. [30] used two sequential CNNs to detect whether calcified lesions were present in a number of large arteries in the chest and neck. Simultaneously the location of a bounding box around the lesion was regressed and thereafter a CNN was used to segment the lesion within the bounding box. In both approaches, application of sequential classifiers substantially reduced the amount of false positive lesion detections [29,30].

Recently, deep learning based methods were proposed for calcium scoring in low-dose chest CT [31,32]. Lessmann et al. [31] used two subsequent CNNs to detect calcifications in the coronary arteries, aorta and cardiac valves. The first CNN exploited dilated convolutions to identify candidate calcification voxels and label them according to their spatial location, and the second CNN identified true calcified voxels among those detected by the first CNN. Note that the voxels were identified instead of the lesions. This was needed to address low-dose CT where high noise levels don't allow region growing of the voxels above the 130 HU extraction threshold.

The aforementioned methods were typically developed and evaluated in a set of scans with uniform image acquisition characteristics. Due to the supervised nature of these methods, they are sensitive to changes in image acquisition parameters and the imaged population. Consequently, a good performance is often suboptimal in CT scans acquired with different acquisition parameters, which limits the clinical applicability. To extend the applicability, in a large-scale multicenter study including CT scans with diverse acquisition protocols, van Velzen et al. [33] evaluated training strategies for the deep learning method proposed by Lessmann et al. [31] for calcium scoring in the coronary arteries and the aorta. The performance was evaluated in CSCT, diagnostic chest CT, radiotherapy planning CT and attenuation correction CT acquired with cardiac perfusion PET. Training with a combination of all available types of CT scans led to excellent agreement in risk categorization between manual and automatic scoring, i.e. linearly weighted Cohen's kappa > 0.9 [28]. This type of generic method eliminates the need for a specialized network for every type of CT, which is practical for wide application in clinical practice.

2.3 Calcium scoring in contrast enhanced scans

For CCTA acquisition an iodine-containing contrast agent is intravenously administered, which enables visualization of blood vessels in the coronary artery

tree. Hence, the current diagnostic purpose of CCTA lies in identification of non-calcified plaque, as well as determination of the presence and quantification of the anatomical significance of coronary artery stenosis. Standard calcium scoring is not applicable to CCTA as the contrast agent in the artery typically exceeds the clinical intensity level threshold of 130 HU (Fig. 3). This led to application of higher detection thresholds of for instance 320 HU [34] or 600 HU [35]. However, due to variations between CCTA scans caused by differences in acquisition protocols, scanners and contrast agents, using the same detection threshold for all subjects does often not lead to the most optimal results (Fig. 3). To address this, the threshold was derived automatically at standardized anatomical locations, e.g. the ascending aorta [36] or the proximal coronary arteries [37].

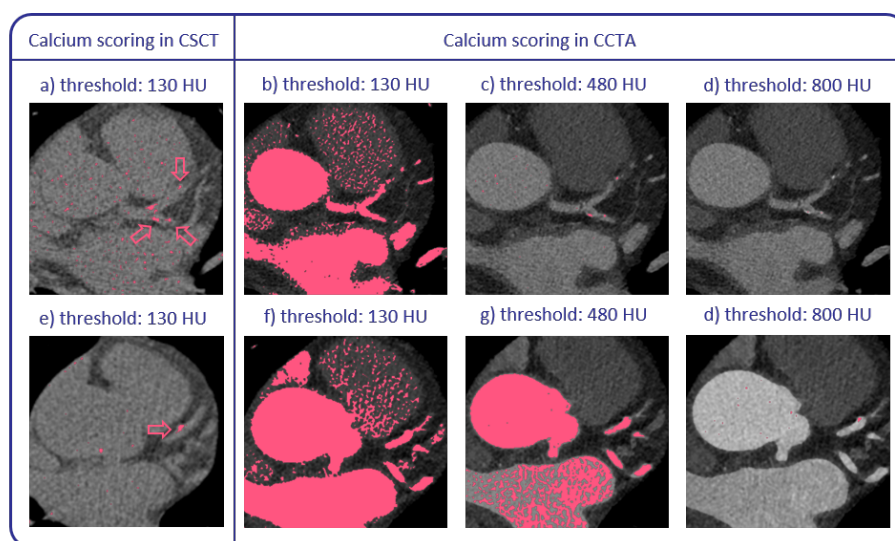


Fig. 3. Paired CSCT and CCTA scans for two different patients (top and bottom). In the CSCT scans, arrows indicate lesions detected by using the clinical intensity level threshold of 130 HU. Different thresholds for calcium scoring in CCTA demonstrate inapplicability of a global threshold and thus the need for adjusted approaches.

Automatic methods for CAC scoring in CCTA typically determine the CAC extraction threshold and localize the coronary arteries (and aorta) by finding their centerlines, thereby allowing detection of CAC lesions in the proximity of the detected centerlines. For example, Teßman et al. [38] derived a threshold from the histogram of the localized vessels and applied this threshold to all voxels in the extracted vessel tree. Subsequently, more complex models were developed in which CAC was defined in relation to the local lumen attenuation values [39,40,41]. Furthermore, Mittal et al. [42] combined machine learning approaches for CAC scoring in CSCT while exploiting the visibility of the coronary arteries in CTA. Namely, the authors trained a random forest classifier based on

handcrafted features to identify CAC lesions along an extracted coronary artery centerline.

Later, deep learning approaches were also utilized. Because extraction of the coronary artery centerlines may be challenging especially in presence of pathology like severe stenosis, Wolterink et al. [43] circumvented this by defining a bounding box around the heart using a deep learning approach [44]. Thereafter, all voxels within the bounding box were classified by an ensemble of four pairs of sequential CNNs, each with either a 2.5D and 3D architecture and varying size of the receptive field. The method showed a high correlation with CSCT reference scores and good agreement of risk categorization [28]. Zreik et al. [45] first extracted coronary artery centerlines and classified the presence of CAC along these centerlines with a combination of a CNN and a recurrent neural network. In this approach CAC was not segmented, but its presence was detected. A later method by Fischer et al. [46] used a similar approach that combined a CNN and a recurrent neural network for CAC detection. While the method showed a high accuracy for CAC lesion detection, their segmentation was not performed and hence, quantification of CAC was not evaluated.

3 Advancing the standard calcium scoring protocol

While the aforementioned methods employed different methodologies to perform automatic calcium scoring, they all closely followed the clinical workflow using the standard definition of arterial calcification. By adjusting this workflow, several automatic methods have been developed that bring calcium scoring to a new level (Fig. 4). For instance, by circumventing the explicit lesion segmentation and directly predicting an Agatston score, methods can be orders of magnitude faster. Furthermore, revisiting the definition of CAC led to a method that provides more reproducible CAC quantification.

3.1 Direct prediction of coronary calcium scores

While the aforementioned methods aimed at calcium scoring in CSCT and other non-contrast CT showing the heart use different approaches, they all follow the manual calcium scoring workflow: Calcified lesions are first identified and thereafter quantified. Although several of the methods show good performance, this comes at a considerable computational cost. Therefore, CAC scoring methods have been proposed that bypass the lesion segmentation step and, instead, directly regress the Agatston score from the CT image [47,48]. Like other methods, these methods focused the analysis on the heart by first defining a ROI. Cano-Espinoza et al. [48] defined a bounding box around the heart using an object-detection method. After defining the ROI, the Agatston score was regressed by a 3D CNN that analyzed the heart volume. This means that, instead of a categorical label as was used in classification, a continuous calcium score is predicted. However, in 14% of the images the heart detection failed and the subsequent analysis could not be performed. In contrast to Cano-Espinoza et al., de Vos et

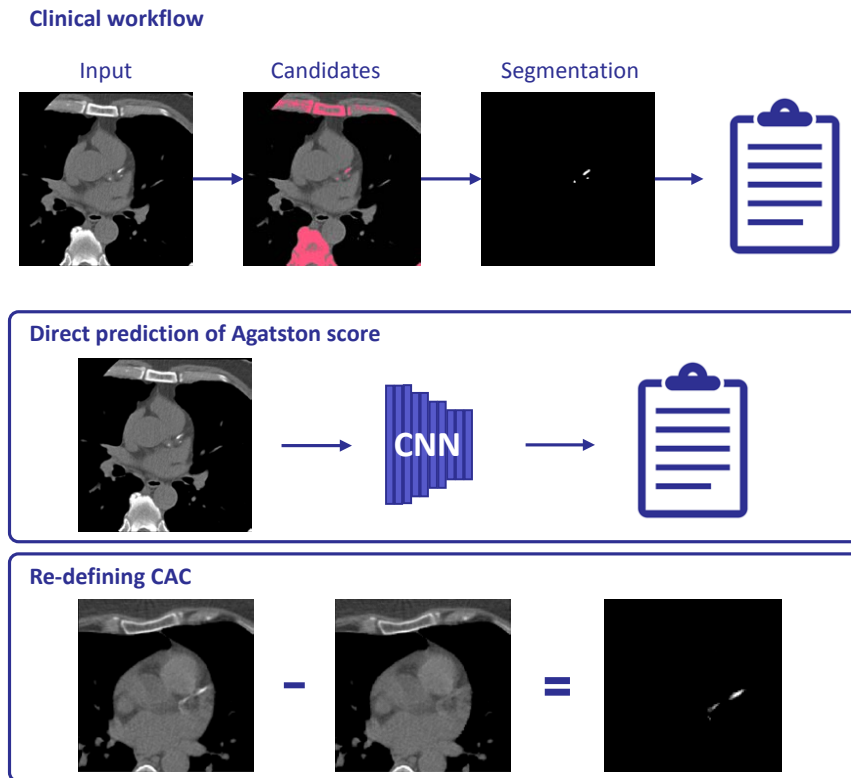


Fig. 4. By augmenting the clinical workflow, several automatic methods have been developed that offer new opportunities.

al. [47] defined the ROI through registration that aligned the analyzed CT with an atlas image that was constructed from CSCT scans. Conventional image registration is typically computationally expensive and slow, defying the purpose of a direct calcium scoring method. Therefore, a deep learning image registration framework [49] was used, which is able to register a 3D image volume in less than a second. Thereafter, the method utilized a 2D CNN architecture to predict an Agatston score in the ROI per image slice. This manner of computation mimicked the clinical calculation of the Agatston score, which is performed in 2D axial image slices (Fig. 5). Next to an accuracy in risk categorization that was comparable or better than for other state-of-the-art calcium scoring methods in cardiac and chest CT [18,31], de Vos et al. [47] showed that their direct calcium scoring method was hundreds of times faster.

3.2 Improving reproducibility

Although coronary calcium scoring is an established and effective method for CVD risk categorization, its interscan reproducibility is limited. For example, in

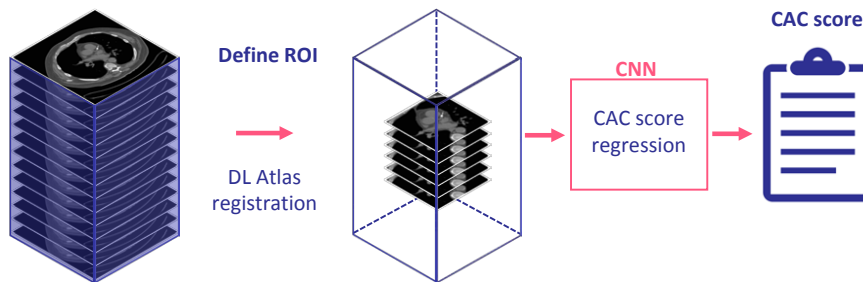


Fig. 5. Direct calcium scoring framework by de Vos et al. [47]: First the region of interest (ROI) containing the heart is determined using deep learning (DL) atlas-registration. Subsequently, the calcium score is regressed with a CNN.

dedicated CSCT scans that are optimized for CAC scoring, the interscan difference in Agatston scores was reported to range from 15% to 41% [50,51,52,53]. In chest scans the reproducibility is even more compromised, due to lack of ECG-triggering and the lower image in-plane resolution. In these scans the reported interscan difference is up to 71%, which led to a difference in risk categorization in 24% of the subjects [54].

Due to the relatively low in-plane resolution especially in non-cardiac CT scans that visualize the heart, the partial volume effect plays a significant role in CAC quantification. The partial volume effect blurs small calcifications so that they remain below the threshold and are missed during segmentation, causing under-estimation of the amount of CAC. Another cause of limited scoring reproducibility is the fact that non-cardiac CTs, like chest CTs, are acquired without ECG-triggering. In these scans extensive cardiac motion can blur lesions or make them invisible.

Increasing the interscan agreement was addressed by many researchers. The earliest approaches adjusted the intensity level threshold for detection of coronary calcifications, instead of using the fixed 130 HU. Groen et al. [55] proposed to use a lesion specific adaptive threshold that is determined using the maximum intensity of the each CAC lesion in non-ECG-triggered CT [55]. In contrast, Song et al. adapted the threshold in a dedicated CSCT protocol based on the intensity of the background in the vicinity of lesions [56]. Another approach aimed at dedicated CSCT protocols was proposed by Sauer et al. [57], who used a mesh-based algorithm to refine the boundaries of a CAC lesion based on the intensity value profile. However, creating a boundary model for small calcifications or those strongly affected by cardiac motion is very challenging, since typically no intensity plateau is reached because of the partial volume effect, which may hamper performance in CT protocols without ECG-triggering. A different method, aimed at non-ECG-triggered protocols, was proposed by Šprem et al. [58], who built on work by Dehmeshki et al. [59]. The authors based their methods on the fact that, due to the limited spatial resolution and cardiac motion, voxels of lesions can

contain a mixture of CAC and other tissues. Using an expectation-maximization algorithm they determined the partial calcium content in each voxel of a CAC lesion and its vicinity. Subsequently, the volume of the lesion was corrected by the partial calcium content.

Development and evaluation of partial volume correction methods is often hampered by the fact that the true amount of calcium in patients cannot be measured non-invasively and thus it is not available. Therefore, most partial volume correction methods either used a phantom for development or used cadaver data. This is problematic for training AI methods that require large training sets. Unfortunately, thus far, only a few methods have been shown to translate well to patient data [58,59].

3.3 Revisiting the clinical definition of arterial calcification

As outlined in Section 3.2, intensity level thresholding contributes to the large interscan reproducibility issues of calcium quantification affected by the partial volume effect and cardiac motion artefacts, especially in non-ECG triggered CT scans.

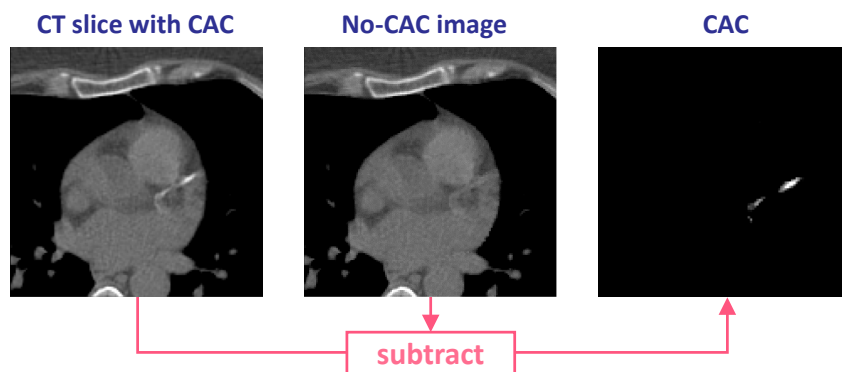


Fig. 6. By defining CAC as the difference between an image visibly containing CAC and a corresponding image without CAC, lesions affected by motion and the partial volume effect can be quantified.

To address this, an automatic CAC scoring method that abandons the clinically used definition of CAC was proposed [60]. Instead of defining lesions using the intensity level threshold, the method defined lesions as the difference between an image visibly containing CAC and a corresponding image without CAC (Fig. 6). Because scan pairs of the same patient, where one scan shows CAC and the other one does not, do not exist, image synthesis with a CycleGAN was used to generate images without CAC from images containing CAC. By using labels that indicate whether an image slice contains CAC, image slices can be sorted

into two domains: a *containing CAC* domain and a domain *without CAC*. Based on these labels a CycleGAN was trained to translate images from one domain to the other and vice versa. By defining the task in this manner, the use of a threshold for detection and segmentation was avoided. Instead, the model itself decides which voxels contain CAC from a higher level of abstraction. Thereby, the method allows quantification of lesions that are partially or completely below the threshold and implicitly corrects for partial volume effect and motion artefacts. The method led to substantially lower relative interscan difference than standard manual calcium scoring. This may lead to improved and more reliable CVD risk prediction.

4 Future directions and conclusions

Recent advances in artificial intelligence research have sparked predictions of a future in which no longer radiologists but advanced computer algorithms read medical images. While this future may still seem distant, AI-based automatic image analysis may much sooner become useful as a supportive tool in the clinic, serving as a second pair of eyes or relieving radiologists and image analysts of tedious tasks. Since manual calcium scoring can be tedious and time consuming, a multitude of AI methods have been developed to automate calcium scoring [10,11] Typically, these AI-based image analysis methods are trained and evaluated on single center studies with high risk for selection biases, and under exclusion of low quality scans. For application in clinical routine, software tools need to be robust to variation in image acquisition parameters and variation in the imaged population. Therefore, ideally large, diverse, well-structured and labeled data sets would be available for the development of new methods and validation of existing techniques. In healthcare, legal barriers often hamper data sharing, and therefore, collecting data for large multi-center evaluation studies is often difficult. This underlines the importance of image analysis challenges for benchmarking the performance of methods. The orCaScore challenge [21] provided an evaluation of several automatic method for calcium scoring in CSCT using multi-center and multi-vendor data. Moreover, a number of methods have proven to be applicable to CTs with different populations or protocols that they were trained on [26,33,61]. This versatility and robustness indicates great potential for broad application in clinical practice.

CAC scoring in CSCT is considered a relatively easy task for an expert and the interobserver agreement is very high in these scans[21]. In non-ECG-synchronized CT, where coronary calcium scoring is more challenging due to e.g. noise, low resolution and motion artefacts, the interobserver variability is typically higher. Similar differences over scans are seen in the performance of the automatic methods. While the orCaScore challenge demonstrated excellent performance of automatic methods in CSCT that closely follow expert performance [62,33,63], methods applied to other CT scans showing the heart were challenged by image artifacts and low resolution. Nevertheless, also in these cases, the per-

formance of several automatic methods closely followed interobserver agreement [31,33,63].

Related to the nature of many AI-driven calcium scoring methods, different approaches were used. Early machine learning methods that were aimed at classifying lesions typically exploit lesion-level labels [13,14,15,16,17,62,64]. Later methods were trained to classify candidate voxels with voxel-level labels [31,33]. Although both approaches require substantial manual labor for obtaining the reference standard, they provide strong supervision, which have been shown to often lead to the best performance compared to other training strategies. Nevertheless, other training strategies also have been successfully used. Methods that directly regress an Agatston score from an image slice, use Agatston scores as labels [48,63]. Because in this approach the labels are defined per image slice instead of per voxel or lesion, the supervision is less strict than with voxel- or lesion labels. However, CAC needs to be manually segmented before a reference Agatston score can be derived, which does not alleviate the workload of defining the reference standard. An explicit advantage of this approach is the gain in speed compared to conventional methods that use segmentation. A different approach, which does not use the clinical CAC definition, uses labels that merely indicate whether CAC is present in an image slice [60]. This manner of annotation is less labor intensive than CAC segmentation. In this approach, the method is trained to derive which voxels contain CAC from information that only indicates whether CAC is present.

For acceptance and application in clinic, the interpretability of a machine learning method is of key importance. Most calcium scoring methods produce a segmentation map, indicating per voxel whether it is part of a calcified lesion, that was used in further quantification. Although the mechanism for prediction of the segmentation map itself is often hidden in the complex algorithm or network, inspection of the calcification segmentation shows the plausibility and accuracy of the calcium scoring result. On the other hand, direct calcium scoring methods only produce an output Agatston score and, as such, act to a greater extent as a black box. De Vos et al.[63] addressed this issue by implementing an optional decision feedback mechanism that shows which parts of the image contributed to the score. Moreover, several types of visualization techniques for CNNs [65,66,67] have been proposed to visualize CNN decision making to improve interpretability of CNNs.

Since the ultimate goal of calcium scoring is to derive a risk of CVD, future research could investigate direct prediction of CVD risk from a CT scan. Hard outcome labels like CVD events or CVD mortality provide a powerful and reliable reference. These labels are defined according to strict clinical protocol and definitions[68], which should make them less subject to interobserver variability. Despite the obvious application potential, this area of research is still in its infancy, likely caused by a combination of a the challenging problem and difficulties of obtaining sufficient data. Given the data sets of limited size that were available for this research, thus far developed methods used a two-step approach, where first features describing the image [69,70] were extracted and

thereafter, a classifier was trained to classify patients according to the outcomes. However, much like in conventional machine learning, the first stage was not directly coupled to the final prediction goal. Incorporating clinical patient data for multitask learning [71] or advanced augmentation techniques [72] may make end-to-end training with a limited dataset feasible.

In the era of precision medicine it has become increasingly important to quantify disease related parameters to provide a complete overview of the patients physical state. Because it requires a substantial manual effort to quantify all relevant parameters from the plethora of information comprised in a CT scan, automation using AI methods can facilitate and speed up the quantification process. Measuring a broad set of CVD parameters, including calcium scores, may aid medical experts in lifting the practice of personalized medicine to a new level. While the value of careful evaluation should not be forgotten, the incorporation of AI into CVD risk prediction is not a change that clinicians should fear, but rather, one that should be embraced.

References

1. G. A. Roth, D. Abate, K. H. Abate, S. M. Abay, C. Abbafati, N. Abbasi, H. Abastabar, F. Abd-Allah, J. Abdela, A. Abdelalim, *et al.*, “Global, regional, and national age-sex-specific mortality for 282 causes of death in 195 countries and territories, 1980–2017: a systematic analysis for the global burden of disease study 2017,” *The Lancet*, vol. 392, no. 10159, pp. 1736–1788, 2018.
2. P. Greenland, M. J. Blaha, M. J. Budoff, R. Erbel, and K. E. Watson, “Coronary calcium score and cardiovascular risk,” *Journal of the American College of Cardiology*, vol. 72, no. 4, pp. 434–447, 2018.
3. C. Iribarren, S. Sidney, B. Sternfeld, and W. S. Browner, “Calcification of the aortic arch: risk factors and association with coronary heart disease, stroke, and peripheral vascular disease,” *JAMA*, vol. 283, no. 21, pp. 2810–2815, 2000.
4. K. R. Nandalur, E. Baskurt, K. D. Hagspiel, M. Finch, C. D. Phillips, S. R. Bollampally, and C. M. Kramer, “Carotid artery calcification on CT may independently predict stroke risk,” *American Journal of Roentgenology*, vol. 186, no. 2, pp. 547–552, 2006.
5. H. S. Hecht, “Coronary artery calcium scanning: past, present, and future,” *JACC: Cardiovascular Imaging*, vol. 8, no. 5, pp. 579–596, 2015.
6. M. J. Budoff, K. Nasir, R. L. McClelland, R. Detrano, N. Wong, R. S. Blumenthal, G. Kondos, and R. A. Kronmal, “Coronary calcium predicts events better with absolute calcium scores than age-sex-race/ethnicity percentiles: MESA (Multi-Ethnic Study of Atherosclerosis),” *Journal of the American College of Cardiology*, vol. 53, no. 4, pp. 345–352, 2009.
7. A. S. Agatston, W. R. Janowitz, F. J. Hildner, N. R. Zusmer, M. Viamonte, and R. Detrano, “Quantification of coronary artery calcium using ultrafast computed tomography,” *Journal of the American College of Cardiology*, vol. 15, no. 4, pp. 827–832, 1990.
8. J. A. Rumberger and L. Kaufman, “A rosetta stone for coronary calcium risk stratification: agatston, volume, and mass scores in 11,490 individuals,” *American Journal of Roentgenology*, vol. 181, no. 3, pp. 743–748, 2003.

9. M. J. Budoff, R. Young, G. Burke, J. Jeffrey Carr, R. C. Detrano, A. R. Folsom, R. Kronmal, J. A. Lima, K. J. Liu, R. L. McClelland, *et al.*, “Ten-year association of coronary artery calcium with atherosclerotic cardiovascular disease (ASCVD) events: the multi-ethnic study of atherosclerosis (MESA),” *European Heart Journal*, vol. 39, no. 25, pp. 2401–2408, 2018.
10. N. Hampe, J. M. Wolterink, S. G. M. Van Velzen, T. Leiner, and I. Išgum, “Machine learning for assessment of coronary artery disease in cardiac CT: a survey,” *Frontiers in Cardiovascular Medicine*, vol. 6, p. 172, 2019.
11. G. Litjens, F. Ciompi, J. M. Wolterink, B. D. de Vos, T. Leiner, J. Teuwen, and I. Išgum, “State-of-the-art deep learning in cardiovascular image analysis,” *JACC: Cardiovascular Imaging*, vol. 12, no. 8, pp. 1549–1565, 2019.
12. H. S. Hecht, P. Cronin, M. J. Blaha, M. J. Budoff, E. A. Kazerooni, J. Narula, D. Yankelevitz, and S. Abbara, “2016 SCCT/STR guidelines for coronary artery calcium scoring of noncontrast noncardiac chest CT scans: A report of the society of cardiovascular computed tomography and society of thoracic radiology,” *Journal of Cardiovascular Computed Tomography*, vol. 11, no. 1, pp. 74–84, 2017.
13. I. Išgum, A. Rutten, M. Prokop, and B. van Ginneken, “Detection of coronary calcifications from computed tomography scans for automated risk assessment of coronary artery disease,” *Medical Physics*, vol. 34, pp. 1450–61, 2007.
14. U. Kurkure, D. R. Chittajallu, G. Brunner, Y. H. Le, and I. A. Kakadiaris, “A supervised classification-based method for coronary calcium detection in non-contrast CT,” *The International Journal of Cardiovascular Imaging*, vol. 26, no. 7, pp. 817–828, 2010.
15. Z. Qian, H. Anderson, I. Marvasty, K. Akram, G. Vazquez, S. Rinehart, and S. Voros, “Lesion-and vessel-specific coronary artery calcium scores are superior to whole-heart agatston and volume scores in the diagnosis of obstructive coronary artery disease,” *Journal of Cardiovascular Computed Tomography*, vol. 4, no. 6, pp. 391–399, 2010.
16. G. Brunner, D. R. Chittajallu, U. Kurkure, and I. A. Kakadiaris, “Toward the automatic detection of coronary artery calcification in non-contrast computed tomography data,” *The International Journal of Cardiovascular Imaging*, vol. 26, no. 7, pp. 829–838, 2010.
17. R. Shahzad, T. van Walsum, M. Schaap, A. Rossi, S. Klein, A. C. Weustink, P. J. de Feyter, L. J. van Vliet, and W. J. Niessen, “Vessel specific coronary artery calcium scoring: an automatic system,” *Academic Radiology*, vol. 20, no. 1, pp. 1–9, 2013.
18. J. M. Wolterink, T. Leiner, R. A. Takx, M. A. Viergever, and I. Išgum, “Automatic coronary calcium scoring in non-contrast-enhanced ECG-triggered cardiac CT with ambiguity detection,” *IEEE Transactions on Medical Imaging*, vol. 34, no. 9, pp. 1867–1878, 2015.
19. S. S. Martin, M. van Assen, S. Rapaka, H. T. Hudson, A. M. Fischer, A. Varga-Szemes, P. Sahbaee, C. Schwemmer, M. A. Gulsun, S. Cimen, P. Sharma, T. J. Vogl, and U. J. Schoepf, “Evaluation of a deep learning based automated CT coronary artery calcium scoring algorithm,” *JACC: Cardiovascular Imaging*, vol. 13, no. 2 Part 1, pp. 524–526, 2020.
20. L. van den Oever, L. Cornelissen, M. Vonder, C. Xia, J. Bolhuis, R. Vliegthart, R. Veldhuis, G. Bock, M. Oudkerk, and P. Van Ooijen, “Deep learning for automated exclusion of cardiac CT examinations negative for coronary artery calcium,” *European Journal of Radiology*, vol. 129, p. 109114, 06 2020.

21. J. M. Wolterink, T. Leiner, B. D. De Vos, J.-L. Coatrieux, B. M. Kelm, S. Kondo, R. A. Salgado, R. Shahzad, H. Shu, M. Snoeren, *et al.*, “An evaluation of automatic coronary artery calcium scoring methods with cardiac CT using the orCaScore framework,” *Medical Physics*, vol. 43, no. 5, pp. 2361–2373, 2016.
22. A. B. De González, M. Mahesh, K.-P. Kim, M. Bhargavan, R. Lewis, F. Mettler, and C. Land, “Projected cancer risks from computed tomographic scans performed in the united states in 2007,” *Archives of Internal Medicine*, vol. 169, no. 22, pp. 2071–2077, 2009.
23. V. A. Moyer, “Screening for lung cancer: US preventive services task force recommendation statement,” *Annals of Internal Medicine*, vol. 160, no. 5, pp. 330–338, 2014.
24. G. González, G. R. Washko, and R. S. J. Estépar, “Automated agatston score computation in a large dataset of non ECG-gated chest computed tomography,” in *2016 IEEE 13th International Symposium on Biomedical Imaging (ISBI)*, pp. 53–57, IEEE, 2016.
25. I. Išgum, M. Prokop, M. Niemeijer, M. A. Viergever, and B. Van Ginneken, “Automatic coronary calcium scoring in low-dose chest computed tomography,” *IEEE Transactions on Medical Imaging*, vol. 31, no. 12, pp. 2322–2334, 2012.
26. I. Išgum, B. D. de Vos, J. M. Wolterink, D. Dey, D. S. Berman, M. Rubeaux, T. Leiner, and P. J. Slomka, “Automatic determination of cardiovascular risk by CT attenuation correction maps in Rb-82 PET/CT,” *Journal of Nuclear Cardiology*, vol. 25, no. 6, pp. 2133–2142, 2018.
27. S. A. M. Gernaat, I. Išgum, B. D. de Vos, R. A. P. Takx, D. A. Young-Afat, N. Rijbergen, D. E. Grobbee, Y. van der Graaf, P. A. de Jong, T. Leiner, D. H. J. van den Bongard, J.-P. Pignol, and H. M. Verkooijen, “Automatic coronary artery calcium scoring on radiotherapy planning CT scans of breast cancer patients: Reproducibility and association with traditional cardiovascular risk factors,” *PloS One*, vol. 11, no. 12, p. e0167925, 2016.
28. J. Cohen, “A coefficient of agreement for nominal scales,” *Educational and Psychological Measurement*, vol. 20, no. 1, pp. 37–46, 1960.
29. I. Išgum, A. Rutten, M. Prokop, M. Staring, S. Klein, J. P. Pluim, M. A. Viergever, and B. van Ginneken, “Automated aortic calcium scoring on low-dose chest computed tomography,” *Medical Physics*, vol. 37, no. 2, pp. 714–723, 2010.
30. K. Chellamuthu, J. Liu, J. Yao, M. Bagheri, L. Lu, V. Sandfort, and R. M. Summers, “Atherosclerotic vascular calcification detection and segmentation on low dose computed tomography scans using convolutional neural networks,” in *2017 IEEE 14th International Symposium on Biomedical Imaging (ISBI 2017)*, pp. 388–391, IEEE, 2017.
31. N. Lessmann, B. van Ginneken, M. Zreik, P. A. de Jong, B. D. de Vos, M. A. Viergever, and I. Išgum, “Automatic calcium scoring in low-dose chest CT using deep neural networks with dilated convolutions,” *IEEE Transactions on Medical Imaging*, vol. 37, pp. 615–625, 2018.
32. N. Lessmann, I. Išgum, A. A. Setio, B. D. de Vos, F. Ciompi, P. A. de Jong, M. Oudkerk, P. T. M. Willem, M. A. Viergever, and B. van Ginneken, “Deep convolutional neural networks for automatic coronary calcium scoring in a screening study with low-dose chest CT,” in *Medical Imaging 2016: Computer-Aided Diagnosis*, vol. 9785, p. 978511, International Society for Optics and Photonics, 2016.
33. S. G. M. van Velzen, N. Lessmann, B. K. Velthuis, I. E. Bank, D. H. van den Bongard, T. Leiner, P. A. de Jong, W. B. Veldhuis, A. Correa, J. G. Terry, *et al.*, “Deep learning for automatic calcium scoring in CT: validation using multiple cardiac CT and chest CT protocols,” *Radiology*, vol. 295, no. 1, pp. 66–79, 2020.

34. J. M. Otton, J. T. Lønborg, D. Boshell, M. Feneley, A. Hayen, N. Sammel, K. Sesel, L. Bester, and J. McCrohon, "A method for coronary artery calcium scoring using contrast-enhanced computed tomography," *Journal of Cardiovascular Computed Tomography*, vol. 6, no. 1, pp. 37–44, 2012.
35. B. Glodny, B. Helmelt, T. Trieb, C. Schenk, B. Taferner, V. Unterholzner, A. Strasak, and J. Petersen, "A method for calcium quantification by means of CT coronary angiography using 64-multidetector CT: very high correlation with Agatston and volume scores," *European Radiology*, vol. 19, no. 7, pp. 1661–1668, 2009.
36. I. Mylonas, M. Alam, N. Amily, G. Small, L. Chen, Y. Yam, B. Hibbert, and B. J. Chow, "Quantifying coronary artery calcification from a contrast-enhanced cardiac computed tomography angiography study," *European Heart Journal—Cardiovascular Imaging*, vol. 15, no. 2, pp. 210–215, 2014.
37. C. W. Pavitt, K. Harron, A. C. Lindsay, R. Ray, S. Zielke, D. Gordon, M. B. Rubens, S. P. Padley, and E. D. Nicol, "Deriving coronary artery calcium scores from CT coronary angiography: a proposed algorithm for evaluating stable chest pain," *The International Journal of Cardiovascular Imaging*, vol. 30, no. 6, pp. 1135–1143, 2014.
38. M. Teßmann, F. Vega-Higuera, B. Bischoff, J. Hausleiter, and G. Greiner, "Automatic detection and quantification of coronary calcium on 3D CT angiography data," *Computer Science-Research and Development*, vol. 26, no. 1-2, pp. 117–124, 2011.
39. D. Dey, V. Y. Cheng, P. J. Slomka, R. Nakazato, A. Ramesh, S. Gurudevan, G. Germano, and D. S. Berman, "Automated 3-dimensional quantification of non-calcified and calcified coronary plaque from coronary CT angiography," *Journal of Cardiovascular Computed Tomography*, vol. 3, no. 6, pp. 372–382, 2009.
40. S. Wesarg, M. F. Khan, and E. A. Firle, "Localizing calcifications in cardiac CT data sets using a new vessel segmentation approach," *Journal of Digital Imaging*, vol. 19, no. 3, pp. 249–257, 2006.
41. W. Ahmed, M. A. de Graaf, A. Broersen, P. H. Kitslaar, E. Oost, J. Dijkstra, J. J. Bax, J. H. Reiber, and A. J. Scholte, "Automatic detection and quantification of the agatston coronary artery calcium score on contrast computed tomography angiography," *The International Journal of Cardiovascular Imaging*, vol. 31, no. 1, pp. 151–161, 2015.
42. S. Mittal, Y. Zheng, B. Georgescu, F. Vega-Higuera, S. K. Zhou, P. Meer, and D. Comaniciu, "Fast automatic detection of calcified coronary lesions in 3D cardiac CT images," in *International Workshop on Machine Learning in Medical Imaging*, pp. 1–9, Springer, 2010.
43. J. M. Wolterink, T. Leiner, B. D. de Vos, R. W. van Hamersvelt, M. A. Viergever, and I. Išgum, "Automatic coronary artery calcium scoring in cardiac CT angiography using paired convolutional neural networks," *Medical Image Analysis*, vol. 34, pp. 123–136, 2016.
44. B. D. de Vos, J. M. Wolterink, P. A. de Jong, T. Leiner, M. A. Viergever, and I. Išgum, "Convnet-based localization of anatomical structures in 3-D medical images," *IEEE Transactions on Medical Imaging*, vol. 36, no. 7, pp. 1470–1481, 2017.
45. M. Zreik, R. W. Van Hamersvelt, J. M. Wolterink, T. Leiner, M. A. Viergever, and I. Išgum, "A recurrent CNN for automatic detection and classification of coronary artery plaque and stenosis in coronary CT angiography," *IEEE Transactions on Medical Imaging*, vol. 38, no. 7, pp. 1588–1598, 2018.

46. A. M. Fischer, M. Eid, C. N. De Cecco, M. A. Gulsun, M. van Assen, J. W. Nance, P. Sahbaee, D. De Santis, M. J. Bauer, B. E. Jacobs, *et al.*, “Accuracy of an artificial intelligence deep learning algorithm implementing a recurrent neural network with long short-term memory for the automated detection of calcified plaques from coronary computed tomography angiography,” *Journal of Thoracic Imaging*, vol. 35, pp. S49–S57, 2020.
47. B. D. de Vos, J. M. Wolterink, T. Leiner, P. A. de Jong, N. Lessmann, and I. Išgum, “Direct automatic coronary calcium scoring in cardiac and chest CT,” *IEEE Transactions on Medical Imaging*, vol. 38, pp. 2127–2138, 2019.
48. C. Cano-Espinosa, G. González, G. R. Washko, M. Cazorla, and R. S. J. Estépar, “Automated agatston score computation in non-ECG gated CT scans using deep learning,” in *Proceedings of SPIE—the International Society for Optical Engineering*, vol. 10574, 2018.
49. B. D. de Vos, F. F. Berendsen, M. A. Viergever, H. Sokooti, M. Staring, and I. Išgum, “A deep learning framework for unsupervised affine and deformable image registration,” *Medical Image Analysis*, vol. 52, pp. 128–143, 2019.
50. R. C. Detrano, M. Anderson, J. Nelson, N. D. Wong, J. J. Carr, M. McNitt-Gray, and D. E. Bild, “Coronary calcium measurements: effect of CT scanner type and calcium measure on rescan reproducibility: MESA study,” *Radiology*, vol. 236, no. 2, pp. 477–484, 2005.
51. S. Mao, H. Bakhsheshi, B. Lu, S. C. Liu, R. J. Oudiz, and M. J. Budoff, “Effect of electrocardiogram triggering on reproducibility of coronary artery calcium scoring,” *Radiology*, vol. 220, no. 3, pp. 707–711, 2001.
52. U. Hoffmann, U. Siebert, A. Bull-Stewart, S. Achenbach, M. Ferencik, F. Moselewski, T. J. Brady, J. M. Massaro, and C. J. O’Donnell, “Evidence for lower variability of coronary artery calcium mineral mass measurements by multi-detector computed tomography in a community-based cohort—consequences for progression studies,” *European Journal of Radiology*, vol. 57, no. 3, pp. 396–402, 2006.
53. L. R. Van Hoe, K. G. De Meerleer, P. P. Leyman, and P. K. Vanhoenacker, “Coronary artery calcium scoring using ecg-gated multidetector CT: effect of individually optimized image-reconstruction windows on image quality and measurement reproducibility,” *American Journal of Roentgenology*, vol. 181, no. 4, pp. 1093–1100, 2003.
54. P. C. Jacobs, I. Išgum, M. J. Gondrie, W. P. T. M. Mali, B. van Ginneken, M. Prokop, and Y. van der Graaf, “Coronary artery calcification scoring in low-dose ungated CT screening for lung cancer: interscan agreement,” *American Journal of Roentgenology*, vol. 194, no. 5, pp. 1244–1249, 2010.
55. J. Groen, H. Dijkstra, M. Greuter, and M. Oudkerk, “Threshold adjusted calcium scoring using CT is less susceptible to cardiac motion and more accurate,” *Medical Physics*, vol. 36, no. 2, pp. 438–446, 2009.
56. Y. Song, B. L. Eck, J. Levi, and D. L. Wilson, “Improved reproducibility of calcium mass score using deconvolution and partial volume correction,” in *Medical Imaging 2019: Biomedical Applications in Molecular, Structural, and Functional Imaging*, vol. 10953, p. 109531O, International Society for Optics and Photonics, 2019.
57. S. C. Saur, H. Alkadhi, L. Desbiolles, G. Székely, and P. C. Cattin, “ACCURATUM: improved calcium volume scoring using a mesh-based algorithm—a phantom study,” *European Radiology*, vol. 19, no. 3, pp. 591–598, 2009.
58. J. Šprem, B. D. De Vos, N. Lessmann, R. W. Van Hamersvelt, M. J. Greuter, P. A. De Jong, T. Leiner, M. A. Viergever, and I. Išgum, “Coronary calcium scoring with partial volume correction in anthropomorphic thorax phantom and screening chest CT images,” *PloS One*, vol. 13, no. 12, p. e0209318, 2018.

59. J. Dehmeshki, X. Ye, H. Amin, M. Abaei, X. Lin, and S. D. Qanadli, "Volumetric quantification of atherosclerotic plaque in CT considering partial volume effect," *IEEE Transactions on Medical Imaging*, vol. 26, no. 3, pp. 273–282, 2007.
60. S. G. M. van Velzen, B. D. de Vos, H. M. Verkooijen, T. Leiner, M. A. Viergever, and I. Išgum, "Coronary artery calcium scoring: Can we do better?," in *Medical Imaging 2020: Image Processing*, vol. 11313, p. 113130G, International Society for Optics and Photonics, 2020.
61. S. A. Gernaat, I. Išgum, B. D. de Vos, R. A. Takx, D. A. Young-Afat, N. Rijnberg, D. E. Grobbee, Y. van der Graaf, P. A. de Jong, T. Leiner, *et al.*, "Automatic coronary artery calcium scoring on radiotherapy planning ct scans of breast cancer patients: reproducibility and association with traditional cardiovascular risk factors," *PLoS One*, vol. 11, no. 12, p. e0167925, 2016.
62. J. M. Wolterink, T. Leiner, R. A. P. Takx, M. A. Viergever, and I. Išgum, "Automatic Coronary Calcium Scoring in Non-Contrast-Enhanced ECG-Triggered Cardiac CT With Ambiguity Detection," *IEEE Transactions on Medical Imaging*, vol. 34, no. 9, pp. 1867–1878, 2015.
63. B. D. de Vos, J. M. Wolterink, T. Leiner, P. A. de Jong, N. Lessmann, and I. Išgum, "Direct automatic coronary calcium scoring in cardiac and chest CT," *IEEE Transactions on Medical Imaging*, 2019.
64. I. Išgum, M. Prokop, M. Niemeijer, M. A. Viergever, and B. van Ginneken, "Automatic coronary calcium scoring in low-dose chest computed tomography," *IEEE Transactions on Medical Imaging*, vol. 31, no. 12, pp. 2322–2334, 2012.
65. M. D. Zeiler and R. Fergus, "Visualizing and understanding convolutional networks," in *European conference on computer vision*, pp. 818–833, Springer, 2014.
66. R. R. Selvaraju, M. Cogswell, A. Das, R. Vedantam, D. Parikh, and D. Batra, "Grad-cam: Visual explanations from deep networks via gradient-based localization," in *Proceedings of the IEEE International Conference on Computer Vision*, pp. 618–626, 2017.
67. Y. Huo, J. G. Terry, J. Wang, V. Nath, C. Bermudez, S. Bao, P. Parvathaneni, J. J. Carr, and B. A. Landman, "Coronary calcium detection using 3d attention identical dual deep network based on weakly supervised learning," in *Medical Imaging 2019: Image Processing*, vol. 10949, p. 1094917, International Society for Optics and Photonics, 2019.
68. W. H. Organization *et al.*, *The ICD-10 classification of mental and behavioural disorders: diagnostic criteria for research*, vol. 2. World Health Organization, 1993.
69. S. G. M. van Velzen, M. Zreik, N. Lessmann, M. A. Viergever, P. A. de Jong, H. M. Verkooijen, and I. Išgum, "Direct prediction of cardiovascular mortality from low-dose chest CT using deep learning," in *Medical Imaging 2019: Image Processing*, vol. 10949, p. 109490X, International Society for Optics and Photonics, 2019.
70. B. D. de Vos, P. A. de Jong, J. M. Wolterink, R. Vliegthart, G. V. Wielingen, M. A. Viergever, and I. Išgum, "Automatic machine learning based prediction of cardiovascular events in lung cancer screening data," in *Medical Imaging 2015: Computer-Aided Diagnosis*, vol. 9414, p. 94140D, International Society for Optics and Photonics, 2015.
71. H. Guo, M. Kruger, G. Wang, M. K. Kalra, and P. Yan, "Multi-task learning for mortality prediction in LDCT images," in *Medical Imaging 2020: Computer-Aided Diagnosis*, vol. 11314, p. 113142C, International Society for Optics and Photonics, 2020.
72. M. Frid-Adar, E. Klang, M. Amitai, J. Goldberger, and H. Greenspan, "Synthetic data augmentation using gan for improved liver lesion classification," in *2018 IEEE*

15th International Symposium on Biomedical Imaging (ISBI 2018), pp. 289–293, IEEE, 2018.